ELSEVIER

An enthalpy-source based lattice Boltzmann model for conduction dominated phase change of pure substances

Dipankar Chatterjee [a,*], Suman Chakraborty [b]

[a] *Department of Mechanical Engineering, B.P. Poddar Institute of Management and Technology, 137, VIP Road, Poddar Vihar, Kolkata-700052, India*
[b] *Department of Mechanical Engineering, Indian Institute of Technology, Kharagpur-721302, India*

Abstract

An enthalpy-source based novel lattice Boltzmann technique is formulated for numerical simulation of conduction-dominated phase change processes of single-component systems. The proposed model is based on a classical lattice Boltzmann scheme for description of internal energy evolution with a fixed-grid enthalpy-based formulation for capturing the phase boundary evolution in an implicit fashion. A single particle density distribution function is used for calculating the thermal variable. The macroscopic energy equation is found to be recovered following the Chapman–Enskog multiscale expansion procedure. It is also found that predictions from the present model agree excellently with results obtained from established analytical/numerical models.
© 2007 Elsevier Masson SAS. All rights reserved.

Keywords: Lattice Boltzmann model; Phase change; Enthalpy formulation

1. Introduction

Freezing of pure substances has been an important area of research over many years. Common applications include solidification of a single-component system in phase change electronics cooling, semiconductor crystal growth, thermal processing in conventional as well as non-traditional manufacturing processes and freezing of ice in food-processing industries, to name a few.

One of the major aspects of understanding freezing of pure substances is the mathematical modeling and numerical simulation of the continuously moving liquid–solid interface and the consequent release of latent heat during the process. In addition, such isothermal phase change processes involve abrupt discontinuity of properties across the interface, which needs to be appropriately taken care of.

Over the years, numerous studies have been executed to model solid–liquid phase transitions, which can broadly be classified as: (a) a grid consideration approach and (b) a latent heat representation approach. The grid consideration approach may be further divided into front tracking [1–5] and fixed grid [6–13] methods. In the front tracking scheme, the position of moving liquid–solid interface is determined in every time step, and separate governing equations for solid and liquid sub-domains are solved, with matching boundary conditions prescribed at the interface. On the other hand, the fixed grid method implicitly captures the interface location by solving an additional differential equation for phase fraction, without necessitating any explicit front tracking. In such approaches, the latent heat is accounted for by employing either a temperature-based formulation or by using an enthalpy-based formulation. The temperature-based approach insists on retaining the temperature as the only state variable. In order to tackle the temperature discontinuity across the interface in isothermal phase change problems, an approximate numerical smoothing needs to be used and a special integration scheme needs to be employed to compute the latent heat [14–16]. The fixed-grid enthalpy-based method, on the other hand, can further be divided into various sub-categories. In the basic enthalpy-based scheme, enthalpy is used as the primary variable and the temperature is calculated from a previously defined enthalpy-temperature rela-

* Corresponding author.
E-mail address: rsdchat@yahoo.co.in (D. Chatterjee).

Nomenclature

b	Number of lattice connection vector		λ	Relaxation factor
c_p	Specific heat		ρ	Density
c	Propagation speed		τ	Relaxation time
$\mathbf{e}_i$	Propagation velocity		ΔH	Latent enthalpy
f_i	Particle distribution function		Δx	Lattice size in x direction
f_i^{eq}	Equilibrium particle distribution function		Δy	Lattice size in y direction
f_l	Liquid fraction		Δt	Time step
H	Total enthalpy		Φ	Energy source term
k_T	Thermal conductivity		Ω	Relaxation parameter
L	Latent heat of fusion		*Subscripts*	
q	Heat flux			
R	Universal gas constant		0	Lattice centre location
St	Stefan number		i	Direction i in a lattice
t	Time		j	Lattice index
T	Temperature		l	Liquid phase
w_i	Weight coefficient		m	Phase changing point
x, y	Coordinate		s	Solid phase
Greek symbols			n	Iteration level
			Superscripts	
α	Thermal diffusivity			
ε	Knudsen number		n	Iteration index

tion. Although this method gives reasonably accurate results for metallic systems solidifying over a range of temperature [17], it is complex and computationally expensive. In the apparent heat capacity method, the latent heat is calculated from the integration of heat capacity with respect to temperature [6,7,18–20]. As the relationship between heat capacity and temperature in isothermal problems involves a Dirac-delta function in theory, the zero-width phase change interval must be approximated by a narrow range of phase change temperatures. Thus, the size of time steps must be small enough so that this temperature range is not overlooked in the calculations. Such drawbacks, however, are not observed in the latent heat source or fictitious heat flow method. In this approach, the latent heat is included in the source term, which is obtained from a prescribed relationship between latent enthalpy and temperature. Although the above simulation strategy has become somewhat standardized over the past few decades, solution of multi-scale melting/solidification problems using this methodology still poses serious challenges, primarily because of the associated computational complexities and time-intensive simulation.

Recently, lattice Boltzmann method (LBM) has emerged with huge potentials for solving partial differential equations associated with fluid flow and heat transfer problems involving morphological development of topologically complicated phase boundaries. This is a relatively new approach that uses simple microscopic kinetic models to simulate complicated macroscopic transport phenomena. Compared with the conventional computational fluid dynamics (CFD) approach, the LBM is simple in form, having high computational performance with regard to stability and accuracy. Further, it is able to handle complex geometry and boundary conditions, and is intrinsically parallelizable. This method has originally been derived from the lattice gas automata (LGA) model [21], and is a specially discretized form of the continuous Boltzmann equation. The LBM effectively simulates physical transport phenomena by employing quasi-particles that populate the domain lattices. The quasi-particles move across the lattice along links connecting neighboring lattice sites, and subsequently undergo collisions upon arrival at a new lattice site. For simulating physical phenomena, the collisions between particles must obey pertinent physical laws. Thus, a fundamental idea of the LBM is to construct simplified kinetic models that incorporate the essential physics of microscopic processes so that the macroscopic averaged properties obey the desired laws. More detailed descriptions of the LBM can be found in the review article [22–24] and the reference books [25,26].

In the context of application of LBM to phase change problems, Wolf-Gladrow [27] first proposed an explicit finite difference formulation, with a relaxation parameter of unity pertaining to the lattice Boltzmann equation for diffusion. De Fabritiis et al. [28] developed a thermal lattice Boltzmann model for liquid–solid phase transition by employing two types of quasiparticles for liquid and solid phases, respectively. Sman et al. [29] developed a one dimensional convection–diffusion scheme for simulating combined heat and mass transfer during cooling of packed cut flowers. Miller et al. [30], subsequently, developed a simple reaction model for liquid–solid phase transition in context of an LBM, with enhanced collisions, using a single type of quasiparticle and a phase field approach. An extended LBM for the heat conduction problem with phase change was developed by Jiaung et al. [31], which can be considered as the first systematic approach of coupling the conventional enthalpy formulation with the discrete lattice Boltzmann equation. However, the above model lacks a thermodynamically-consistent

accounting of latent heat evolution, and therefore, is not very much suitable to be extended to more involved phase transformation problems involving multi-component systems.

Aim of the present work is to develop a hybrid LBM, capable of thermodynamically-consistent representation of phase boundary evolution during conduction-dominated solidification of a single-component system. For this purpose, an enthalpy-based LBM is formulated, in conjunction with an appropriate enthalpy updating scheme, so as to ensure a temperature field that is consistent with local phase change considerations. The model is subsequently tested to simulate formation of ice in a two dimensional domain, as a representative problem. The results obtained from the lattice Boltzmann simulation are finally compared with finite volume simulation results, to establish authenticity of the proposed LBM for solving complex phase change problems.

2. Mathematical formulation

2.1. Continuum model

The equivalent single-phase macroscopic thermal energy conservation equation, in terms of total enthalpy, can be written as:

$$\partial_t(\rho H) = \nabla \cdot (k_T \nabla T) \tag{1}$$

where ρ is the density, H is the total enthalpy, k_T is the thermal conductivity and T is the macroscopic temperature. The total enthalpy, H, can further be decomposed into two components, namely, the sensible enthalpy and the latent enthalpy, and accordingly can be written as: $H = c_p T + \Delta H$, where c_p is the constant pressure specific heat. In order to establish a single-component phase change, the latent heat contribution is specified as a function of temperature, T, and the resulting expression is as:

$$\Delta H = f(T) \begin{cases} L & \text{for } T \geqslant T_m \\ 0 & \text{for } T < T_m \end{cases} \tag{2}$$

where T_m is the freezing temperature of the pure substance and ΔH is the latent enthalpy content of a control volume; L being the corresponding latent heat of freezing. Accordingly, Eq. (1) simplifies to the following form:

$$\partial_t(\rho c_p T) = \nabla \cdot (k_T \nabla T) - \partial_t(\rho \Delta H) \tag{3}$$

in which the latent heat appears as a heat source term in the governing equation. For constant thermophysical properties, Eq. (3) can be written as:

$$\partial_t T = \alpha \nabla^2 T + \Phi \tag{4}$$

where, $\Phi = -(1/c_p)\partial_t \Delta H$, can be regarded as a latent heat source term in Eq. (4).

2.2. Lattice Boltzmann model

As mentioned earlier, the LBM originates from a microscopic description for the evolution of a non-dimensional particle distribution function, following the classical Boltzmann

equation. The particle distribution function, $f_i(\mathbf{x}, t)$, is the probability of finding a particle at location $\mathbf{x}$ and time t, moving in direction i with velocity $\mathbf{e}_i = \Delta \mathbf{x}_i / \Delta t$ along the lattice link and is given by the lattice Boltzmann equation (LBE) as:

$$\partial_t f_i(\mathbf{x}, t) + \mathbf{e}_i \cdot \nabla f_i(\mathbf{x}, t) = \Omega_i(f) \tag{5}$$

where $\Omega_i(f)$ represents the local change in the particle distribution owing to particle collision. A simple single time relaxation BGK approximation [32] leads to the following form of the linearized collision operator:

$$\Omega_i(f) = -\frac{1}{\tau}\big[f_i(\mathbf{x}, t) - f_i^{\text{eq}}(\mathbf{x}, t)\big] \tag{6}$$

where τ is the relaxation time and $f_i^{\text{eq}}(\mathbf{x}, t)$ is the equilibrium distribution function.

Introduction of the above collision operator in the LBE gives the celebrated LBGK model:

$$\partial_t f_i(\mathbf{x}, t) + \mathbf{e}_i \cdot \nabla f_i(\mathbf{x}, t) = -\frac{1}{\tau}\big[f_i(\mathbf{x}, t) - f_i^{\text{eq}}(\mathbf{x}, t)\big] \tag{7}$$

Eq. (7) can be integrated in time to yield the evolution equation of the particle distribution function as:

$$\begin{aligned} f_i(\mathbf{x} + \mathbf{e}_i \Delta t, t + \Delta t) \\ = f_i(\mathbf{x}, t) - (\Delta t/\tau)\big(f_i(\mathbf{x}, t) - f_i^{\text{eq}}(\mathbf{x}, t)\big) \end{aligned} \tag{8}$$

The pertinent macroscopic physical quantities, subsequently, can be obtained from the above particle distribution function information. For instance, for a heat diffusion problem, the temperature can be obtained as:

$$T(\mathbf{x}, t) = \sum_{i=0}^{b} f_i(\mathbf{x}, t) \tag{9}$$

where b is the number of lattice connection vectors.

The equilibrium distribution function, appearing in Eq. (7), can be described as:

$$f_i^{\text{eq}}(\mathbf{x}, t) = w_i T(\mathbf{x}, t) \tag{10}$$

where w_i represents a weight factor along the direction i. For a two dimensional nine velocity (d2q9) model, the discrete velocities and weight coefficients assume the following forms:

$$\mathbf{e}_i = \begin{cases} (0, 0), & i = 0 \\ (\pm 1, 0)c, (0, \pm 1)c, & i = 1, 2, 3, 4 \\ (\pm 1, \pm 1)c, & i = 5, 6, 7, 8 \end{cases} \quad \text{and}$$

$$w_i = \begin{cases} 4/9, & i = 0 \\ 1/9, & i = 1, 2, 3, 4 \\ 1/36, & i = 5, 6, 7, 8 \end{cases} \tag{11}$$

where $c \ (= \Delta \mathbf{x}/\Delta t = \sqrt{3RT})$ is the characteristic speed.

The discrete velocities (i.e., values of $\mathbf{e}_i$) and the weight coefficients (i.e., values of w_i) are determined so as to recover the continuum governing equation from the LBM in the long-wavelength and low-frequency limit. Therefore, the necessary conditions imposed on e_i and w_i are as follows [33]:

$$\sum_i w_i = 1$$

$$\sum_i w_i e_{i\alpha} = 0$$

$$\sum_i w_i e_{i\alpha} e_{i\beta} = \frac{1}{3} c^2 \delta_{\alpha\beta} \tag{12}$$

and the components of the grid velocities obey the following relations:

$$\sum_{i=0}^{8} \mathbf{e}_i = 0$$

$$\sum_{i=1}^{4} e_{i\alpha} e_{i\beta} = 2c^2 \delta_{\alpha\beta}$$

$$\sum_{i=5}^{8} e_{i\alpha} e_{i\beta} = 4c^2 \delta_{\alpha\beta} \tag{13}$$

where $\delta_{\alpha\beta}$ is the Kronecker delta.

The equilibrium distribution function satisfies the following relations:

$$\sum_{i=0}^{8} f_i^{\mathrm{eq}} = \sum_{i=0}^{8} w_i T = T$$

$$\sum_{i=0}^{8} e_{i\alpha} f_i^{\mathrm{eq}} = 0$$

$$\sum_{i=0}^{8} e_{i\alpha} e_{i\beta} f_i^{\mathrm{eq}} = \frac{1}{3} c^2 T \delta_{\alpha\beta} \tag{14}$$

In order to develop a phase change model consistent with the above framework, the heat source term (Φ) of Eq. (4) needs to be retained in the discretized Boltzmann equation. Thus, the discretized phase change LBM takes the form [31]:

$$f_i(\mathbf{x} + \mathbf{e}_i \Delta t, t + \Delta t) = f_i(\mathbf{x}, t) - (\Delta t/\tau)\big(f_i(\mathbf{x}, t) - f_i^{\mathrm{eq}}(\mathbf{x}, t)\big)$$
$$+ \Delta t w_i \Phi \tag{15}$$

It is found that invoking the Chapman–Enskog expansion, Eq. (14) recovers the macroscopic energy equation (4) (see Appendix A) for the following modeling of thermal diffusivity [29]:

$$\alpha = \frac{c^2}{6}(2\tau - \Delta t) \tag{16}$$

It needs to be noted here that the term ΔH appearing in Eq. (15), through the source term Φ, needs to be posed in consistency with microscopic phase change considerations, in order to avoid thermodynamically inconsistent solutions. In fact, for accurate prediction of the liquid fraction, ΔH of each computational cell needs to be updated according to the predicted macroscopic value of temperature each iteration within a time step, for successful implementation of the present hybrid method. Such an updating effectively attempts to neutralize the difference in the nodal temperatures predicted by the internal energy density distribution function, and that dictated by the

phase change considerations. For that purpose, a modified updating scheme, in accordance with the formulation of Brent et al. [34], is used, which is of the form:

$$[\Delta H]_{n+1} = [\Delta H]_n + \lambda\big[\{h\}_n - F^{-1}\{\Delta H\}_n\big] \tag{17}$$

where n is the iteration level characterizing the updation stage, h is the enthalpy of the concerned computational cell, and λ is a suitable relaxation factor to smoothen convergence. In the above formulation, $F^{-1}(\Delta H)$ is the inverse latent heat function, which needs to be constituted in consistency with microscopic phase change considerations. A general prescription of the above function, consistent with pertinent rules of phase transformation, is outlined in [35]. For a phase changing pure material $F^{-1}(\Delta H)$ obtains a simplified form of:

$$F^{-1}(\Delta H) = c_p T_m \tag{18}$$

3. Numerical implementation

3.1. Boundary conditions

A boundary can be introduced to a lattice Boltzmann model by selecting the grid sites where the boundary is to be set and evolving the particle distribution function in a different manner at these sites. Two types of boundary conditions are described for the present context, one is prescribed temperature and another one is the prescribed heat flux.

Following Fig. 1, a Dirichlet boundary condition (i.e. prescribed temperature) can be imposed on the left wall (temperature T_0), for example. To determine f_1, f_5, and f_8, first Eq. (9) is invoked as:

$$f_1 + f_5 + f_8 = T_0 - (f_0 + f_2 + f_3 + f_4 + f_6 + f_7) \tag{19}$$

Now, applying the bounce back rule at the wall, $f_1 = f_3 - (f_3^{\mathrm{eq}} - f_1^{\mathrm{eq}})$ and $f_5 = f_7 - (f_7^{\mathrm{eq}} - f_5^{\mathrm{eq}})$, one obtains:

$$f_1 = f_3$$
$$f_5 = f_7$$
$$f_8 = T_0 - (f_0 + f_2 + 2f_3 + f_4 + f_6 + 2f_7) \tag{20}$$

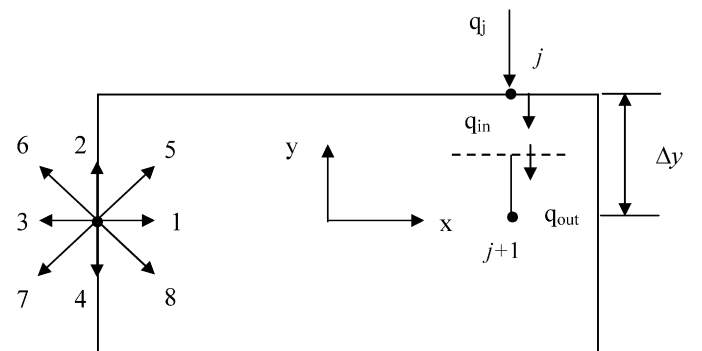The boundary conditions for other walls follow the same procedure.

Fig. 1. Schematic plot of particle streaming and boundary condition for a d2q9 model.

A Neumann boundary condition (i.e. prescribed heat flux) can be implemented by following a conventional control volume based formulation. Applying an energy balance to the boundary lattice j (refer to Fig. 1),

$$\rho c_p \int_j^{j+1/2} \int_t^{t+\Delta t} \frac{\partial T}{\partial t} \, dt \, dV = \int_A \int_t^{t+\Delta t} (q_{\text{in}} - q_{\text{out}}) \, dt \, dA \qquad (21)$$

where $q_{\text{in}} = q_j$ is the prescribed heat flux and q_{out} is the flux leaving the control volume (which can be described by Fourier's law). Hence, Eq. (21) becomes:

$$\rho c_p \frac{\Delta y}{2} (T_j^{n+1} - T_j^n) = \int_t^{t+\Delta t} \left[q_j - \frac{k_T (T_j - T_{j+1})}{\Delta y} \right] dt \qquad (22)$$

where superscripts n and $n+1$ represent time levels t and $t + \Delta t$, respectively. Applying an explicit scheme, the following linear algebraic equation yields form Eq. (22):

$$a_j T_j^{n+1} = (a_j - a_{j+1}) T_j^n + a_{j+1} T_{j+1}^n + q_j \qquad (23)$$

where $a_j = \rho c_p \Delta y / 2\Delta t$ and $a_{j+1} = k_T / \Delta y$. Eq. (23) can be utilized to convert a prescribed heat flux boundary condition, as an equivalent pseudo-isothermal boundary condition, which in turn, can be implemented identical to the generalized formulation for incorporation of Dirichlet type boundary condition, described as above.

3.2. Overall solution algorithm

In a typical simulation, the initial temperature distribution, $T(\mathbf{x}, 0)$, along with the liquid-fraction field, $f_l(\mathbf{x}, 0)$, are prescribed as initial conditions. The initial distribution function, $f_i(\mathbf{x}, 0)$, is obtained by using one term in its Knudsen expansion, i.e., $f_i(\mathbf{x}, 0) = f_i^{\text{eq}}(\mathbf{x}, 0)$. The distribution function is then evolved according to Eq. (15). The following pseudo code demonstrates an overall procedure for implementing the present hybrid LBM:

```
Start Program
Read the Geometry
Set Initial Temperature and Liquid Fraction Distributions
Calculate Initial Distribution Function
Loop for Time Steps
{
    1. Impose Boundary Conditions
    2. Propagate Particles (Streaming)
    3. Calculate Equilibrium Distribution Functions
    4. Calculate Relaxation
    5. Obtain Temperature and Liquid Fraction Fields
    6. Update Nodal Enthalpy
    7. Go Back to Step 1 Until Convergence
}
Obtain Macroscopic Variables
End Program
```

It can be noted here that convergence in inner iterations is declared if the following criterion is satisfied:

$$\min \left(\left| \frac{T^{n+1} - T^n}{T^n} \right|, \left| \frac{\Delta H^{n+1} - \Delta H^n}{\Delta H^n} \right| \right) \leqslant 10^{-8} \qquad (24)$$

4. Results and discussion

For validation of the numerical code developed, first a simple transient 2-D heat conduction problem, with known analytical solutions [36], is solved. An excellent agreement is found between the present solutions and classical analytical solutions, which has been omitted here for the purpose of brevity. Subsequently, the present code is employed to simulate an ice block freezing problem, for which the geometrical and physical parameters are taken from Prapainop and Maneeratana [37]. Fig. 2 shows the problem domain (0.26 m × 0.13 m with an aspect ratio 2), initially ($t = 0$) containing liquid water at a uniform temperature T_i, which is greater than or equal to the freezing temperature T_m. The left ($x = 0$) and bottom ($y = 0$) boundary temperatures are fixed to a temperature T_0, which is below the phase change temperature, T_m. Solidification begins along the left and bottom boundary surfaces and propagates into the material. For simulation purpose the parameters are normalized subsequently to cope up with the LBM. Accordingly, we set, $T_i = 3$, $T_0 = -1$ and $T_m = 0$. Further, the thermal diffusivity ratio for the liquid and solid phase (α_l / α_s) is taken as 0.1 [38] and the relaxation times are set to be different for the liquid and solid phases. For the region ($0 < f_l < 1$), the relaxation time can be expressed by the relation: $\tau = 0.5 + (\alpha_l / \alpha_s)(\tau_s - 0.5) f_l$, where τ_s is the relaxation time corresponding to the solid diffusivity, α_s [31]. The other parameters are set as follows: $\Delta x = \Delta t = 1$, $\alpha_s = 1$, $k_{Tl}/k_{Ts} = 0.25$ with $k_{Ts} = 2$, $c_{pl}/c_{ps} = 2$ with $c_{ps} = 0.5$, $L = 1$, and Stefan number $St = c_{ps}(T_m - T_0)/L = 0.5$. Numerical simulations are performed with a 64 × 32 uniform grid system in a 9 speed square lattice (d2q9) over 3×10^5 time steps, corresponding to 1 min of physical time.

Fig. 3 shows the predicted isotherms at a time of 5 h. The temperature distributions clearly show heat transfer through both exposed edges (left and bottom), causing curved temperature profiles, which clearly exhibit steep gradients of temperature along the diagonal lines. The rate of heat transfer, characterized by these isotherms, strongly depends on the diffusivity ratio in the respective phases as well as on the prevailing temperature gradients, which are implicitly influenced by dynamic locations of the freezing front. Incidentally, the freezing front advances along the $x = y$ diagonal line, which is obvious from the problem geometry and imposed boundary conditions. A time history of temperature at the innermost cell, which freezes last, is illustrated in Fig. 4. The time history exhibits characteristic temperature gradients over liquid and solid re-
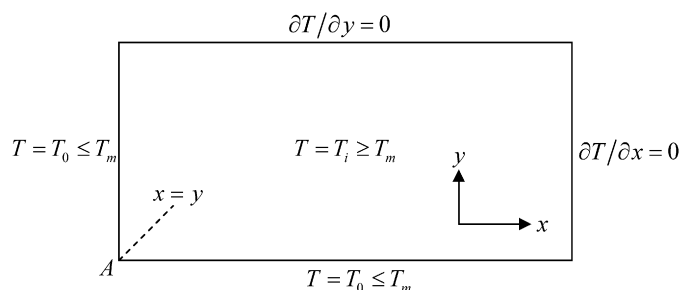

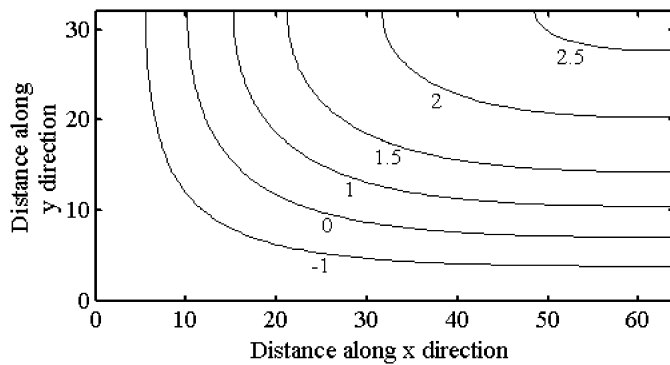Fig. 2. Schematic of isothermal freezing of ice-block.
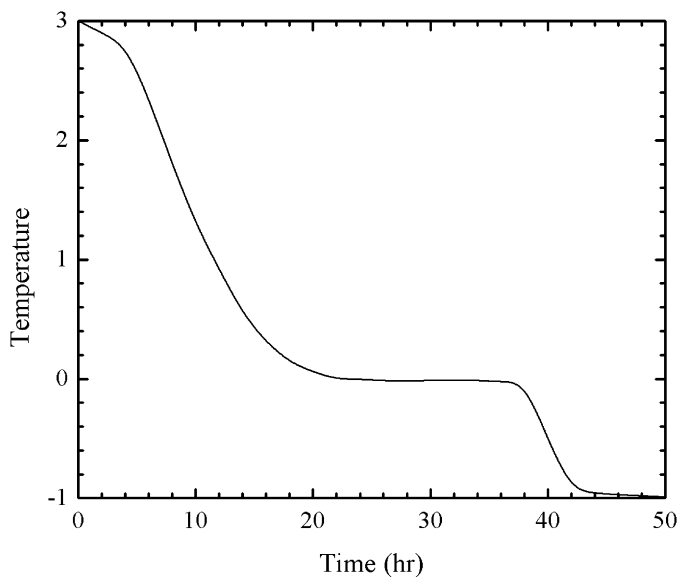
Fig. 3. Temperature contour at time = 5 h.

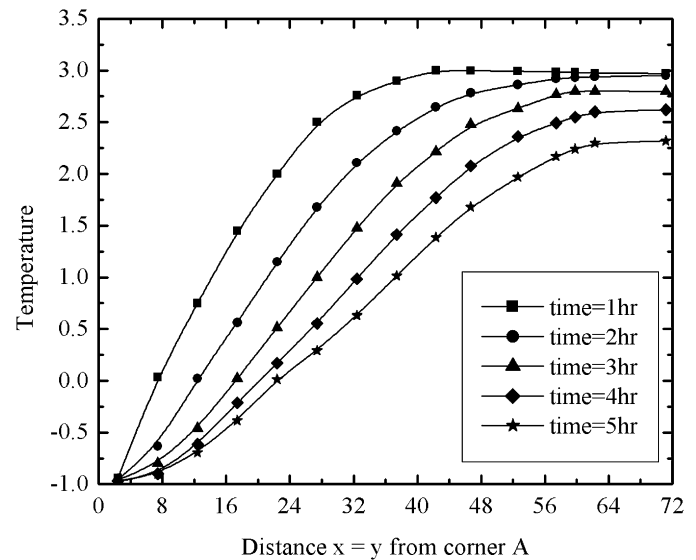Fig. 4. Temperature history of the innermost cell.

Fig. 5. Temperature plot at different time along the line $x = y$.

Table 1
A comparison of computational performance of the present model and a continuum-based model, in terms of simulation speed and grid size requirements

Method of solution	Grid requirement	CPU time (h)
Continuum approach (fully implicit scheme) [37]	104×52 Aspect ratio: 2	6 corresponding to 5 h simulation time
Enthalpy based LB method	64×32 Aspect ratio: 2	4 corresponding to 5 h simulation time on a PIV 2.8 GHz PC

Table 2
A summary of grid sensitivity study

Grid size	% deviation in liquid fraction	% deviation in temperature
48×24	0.92	1.48
56×28	1.25	1.64
82×41	1.36	1.96

Note: The percentage error is calculated using $|\phi - \phi_z|/\phi$, where ϕ_z is based on 64×32 lattices.

gions, and a 'plateau' indicating isothermal changes in phase over a range of time. It takes around 46 hours for the water to fully freeze, which is consistent with the real manufacturing cycle which is around 48–50 hours [37]. The finite volume prediction for the same in [37] is 42 hours, which shows that the present LBM based computation is more close to the real value compared with the finite volume prediction. Typical temperature variations along the line $x = y$, for different times, are depicted in Fig. 5. Abrupt changes in temperature gradient represent locations at which a change in phase occurs, corresponding to a specific instance of time. As time progresses, this location appears to be further away from the lower left corner of the domain, indicating the dynamic nature of front propagation. Further, a qualitative comparison of the results presented in Fig. 5 with that reported in [37] shows that the nature of temperature variations is consistent, which in turn establishes the validity of the proposed algorithm.

Table 1 shows a comparison of the present model with the continuum method, in terms of grid requirements and CPU time. The comparison shows that the present method requires a considerably less CPU time for effective simulation of generic problems benchmarked in the contemporary literature. A com-

prehensive grid sensitivity study is also carried out, and the outcome is presented in Table 2. It is revealed that the percentage error with respect to liquid fraction and temperature predictions does not change appreciably with grid refinement, beyond a threshold mesh distribution, which is much coarser than typical refined mesh structures necessary for implementation of continuum-based classical models of phase transition. This, in turn, demonstrates the effectiveness of the proposed method as a practical tool for numerical simulation of solid–liquid phase transition problems.

5. Conclusions

Phase change phenomenon of a single-component system is computationally handled by a novel enthalpy-based lattice Boltzmann model. A modified latent heat updating procedure

is integrated with the internal energy evolution equation, for capturing the phase change effects. Results obtained from the present study are consistent with analytical as well as numerical results reported in the literature. The present model can also be easily extended to the solution of multicomponent solidification problems, by judiciously modifying the latent heat updating function. Future efforts will be devoted to include the effects of thermo-solutal convection in a generalized lattice Boltzmann framework, with a vision of establishing more computationally elegant approaches for solving more complicated phase change problems.

Appendix A

To perform the multi-scale Chapman–Enskog expansion in the present context we must first expand the population function with respect to the Knudsen number ε ($\ll 1$) as:

$$f_i = f_i^{(0)} + \varepsilon f_i^{(1)} + \mathrm{O}(\varepsilon^2) \tag{A.1}$$

Since the diffusion equation is a linear differential equation, the population function is expanded up to linear terms in the small expansion parameter ε. Further, as the diffusion is a slow process on large spatial scales, the following scaling is introduced to expand the time and space derivatives [31]:

$$\partial_t \approx \varepsilon^2 \partial_{2t}$$
$$\partial_x \approx \varepsilon \partial_{1x} \tag{A.2}$$

Next the population function $f_i(\mathbf{x} + \mathbf{e}_i \Delta t, t + \Delta t)$ is expanded in a Taylor series to obtain:

$$
\begin{aligned}
& f_i(\mathbf{x} + \mathbf{e}_i \Delta t, t + \Delta t) - f_i(\mathbf{x}, t) \\
& \simeq \Big[\Delta t \partial_t + \Delta t e_{i\alpha} \partial_\alpha + \tfrac{1}{2} (\Delta t)^2 \{ e_{i\alpha} \partial_\alpha (e_{i\beta} \partial_\beta + \partial_t) \\
& \quad + \partial_t (e_{i\alpha} \partial_\alpha + \partial_t) \} \Big] f_i(\mathbf{x}, t) + \mathrm{O}(\Delta t^3)
\end{aligned} \tag{A.3}
$$

Substituting Eqs. (A.1)–(A.3) into Eq. (15) and in the consecutive order of parameters ε, it is possible to arrive at the following equations:

$$
\begin{aligned}
& \Big\{ \varepsilon^2 \partial_{2t} + e_{i\alpha} \varepsilon \partial_{1\alpha} + \tfrac{1}{2} (\Delta t) e_{i\alpha} \varepsilon \partial_{1\alpha} [e_{i\beta} \varepsilon \partial_{1\beta} + \varepsilon^2 \partial_{2t}] \\
& \quad + \tfrac{1}{2} (\Delta t) \varepsilon^2 \partial_{2t} [e_{i\alpha} \varepsilon \partial_{1\alpha} + \varepsilon^2 \partial_{2t}] \Big\} \\
& \times \big(f_i^{(0)} + \varepsilon f_i^{(1)} \big) = -\tfrac{1}{\tau} \big(f_i^{(0)} + \varepsilon f_i^{(1)} - f_i^{(0)} \big) + w_i \Phi
\end{aligned} \tag{A.4}
$$

$$\mathrm{O}(\varepsilon^0): \quad f_i^{(0)} = f_i^{\mathrm{eq}} \tag{A.5}$$

$$\mathrm{O}(\varepsilon^1): \quad \partial_{1t} f_i^{(0)} + \partial_{1\alpha} e_{i\alpha} f_i^{(0)} = -\tfrac{1}{\tau} f_i^{(1)} \tag{A.6}$$

where the notation $(\partial_{1x})_\alpha = \partial_{1\alpha}$ has been used. Truncating the terms with order of magnitude larger than $\mathrm{O}(\Delta t^2)$ and $\mathrm{O}(\varepsilon^3)$, one obtain:

$$
\begin{aligned}
& \Big[\varepsilon^2 \partial_{2t} + e_{i\alpha} \varepsilon \partial_{1\alpha} + \tfrac{1}{2} (\Delta t) \varepsilon^2 e_{i\alpha} e_{i\beta} \partial_{1\alpha} \partial_{1\beta} \Big] \big(f_i^{(0)} + \varepsilon f_i^{(1)} \big) \\
& = -\tfrac{1}{\tau} \varepsilon f_i^{(1)} + w_i \Phi
\end{aligned} \tag{A.7}
$$

Summing Eq. (A.7) over all states gives:

$$
\begin{aligned}
& \sum_i \varepsilon^2 \partial_{2t} f_i + \sum_i e_{i\alpha} \varepsilon \partial_{1\alpha} \big[f_i^{(0)} + \varepsilon f_i^{(1)} \big] \\
& \quad + \tfrac{1}{2} (\Delta t) \sum_i \varepsilon^2 e_{i\alpha} e_{i\beta} \partial_{1\alpha} \partial_{1\beta} \big[f_i^{(0)} + \varepsilon f_i^{(1)} \big] \\
& = -\tfrac{1}{\tau} \varepsilon \sum_i f_i^{(1)} + \Phi \sum_i w_i
\end{aligned} \tag{A.8}
$$

Recognizing that the population functions satisfy the following relations:

$$\sum_i f_i^{(\alpha)} = \sum_i e_{i\alpha} f_i^{(\alpha)} = 0 \quad \text{for } \alpha = 1, 2 \tag{A.9}$$

Eq. (A.8) assumes the following form:

$$
\begin{aligned}
& \sum_i \varepsilon^2 \partial_{2t} f_i + \varepsilon \partial_{1\alpha} \sum_i e_{i\alpha} \varepsilon f_i^{(1)} \\
& \quad + \tfrac{1}{2} (\Delta t) \varepsilon^2 \partial_{1\alpha} \partial_{1\beta} \sum_i e_{i\alpha} e_{i\beta} f_i^{(0)} = \Phi
\end{aligned}
$$

$$
\begin{aligned}
\Rightarrow \quad & \varepsilon^2 \partial_{2t} \sum_i f_i + \varepsilon \partial_{1\alpha} \sum_i e_{i\alpha} (-\tau e_{i\alpha} \partial_\alpha f_i - \tau \partial_t f_i) \\
& + \tfrac{1}{2} (\Delta t) \varepsilon^2 \partial_{1\alpha} \partial_{1\beta} \sum_i e_{i\alpha} e_{i\beta} f_i^{(0)} = \Phi
\end{aligned}
$$

$$
\begin{aligned}
\Rightarrow \quad & \partial_t \sum_i f_i + \varepsilon \partial_{1\alpha} \sum_i e_{i\alpha} \big[-\tau e_{i\alpha} \varepsilon \partial_{1\alpha} \big(f_i^{(0)} + \varepsilon f_i^{(1)} \big) \\
& - \tau \varepsilon^2 \partial_{2t} \big(f_i^{(0)} + \varepsilon f_i^{(1)} \big) \big] \\
& + \tfrac{1}{2} (\Delta t) \varepsilon^2 \partial_{1\alpha} \partial_{1\beta} \sum_i e_{i\alpha} e_{i\beta} f_i^{(0)} = \Phi
\end{aligned}
$$

$$
\begin{aligned}
\Rightarrow \quad & \partial_t \sum_i f_i - \tau \varepsilon^2 \partial_{1\alpha} \partial_{1\beta} \sum_i e_{i\alpha} e_{i\beta} f_i^{(0)} \\
& + \tfrac{1}{2} (\Delta t) \varepsilon^2 \partial_{1\alpha} \partial_{1\beta} \sum_i e_{i\alpha} e_{i\beta} f_i^{(0)} = \Phi
\end{aligned}
$$

$$\Rightarrow \quad \partial_t T - \tfrac{\tau}{3} c^2 \nabla^2 T + \tfrac{\Delta t}{6} c^2 \nabla^2 T = \Phi$$

$$\Rightarrow \quad \partial_t T = \Big[\tfrac{c^2}{6} (2\tau - \Delta t) \Big] \nabla^2 T + \Phi = \alpha \nabla^2 T + \Phi \tag{A.10}$$

Hence the macroscopic energy equation (4) is recovered through the Chapman–Enskog expansion.

References

[1] B. Rubinsky, E.G. Cravahlo, A finite element method for the solution of one-dimensional phase change problems, Int. J. Heat Mass Transfer 24 (1981) 1987–1989.

[2] V. Voller, M. Cross, Accurate solutions of moving boundary problems using the enthalpy method, Int. J. Heat Mass Transfer 24 (1981) 545–556.

[3] V. Voller, M. Cross, An explicit numerical method to track a moving phase change front, Int. J. Heat Mass Transfer 26 (1983) 147–150.

[4] J.A. Weaver, R. Viskanta, Freezing of liquid saturated porous media, Int. J. Heat Mass Transfer 33 (1986) 2721–2734.

[5] H.G. Askar, The front tracking scheme for the one-dimensional freezing problem, Int. J. Numer. Methods Eng. 24 (1987) 859–869.

[6] G. Comini, S.D. Guidice, R.W. Lewis, O.C. Zienkiewicz, Finite element solution of non-linear heat conduction problems with special reference to phase change, Int. J. Numer. Methods Eng. 8 (1974) 613–624.

[7] K. Morgan, R.W. Lewis, O.C. Zienkiewicz, An improved algorithm for heat conduction problems with phase change, Int. J. Numer. Methods Eng. 12 (1978) 1191–1195.

[8] J. Roose, O. Storrer, Modelization of phase changes by fictitious heat flow, Int. J. Numer. Methods Eng. 20 (1984) 217–225.

[9] A.J. Dalhuijsen, A. Segal, Comparison of finite element techniques for solidification problems, Int. J. Numer. Methods Eng. 23 (1986) 1807–1829.

[10] Q.T. Pham, The use of lumped capacitance in the finite-element solution of heat conduction problems with phase change, Int. J. Heat Mass Transfer 29 (1986) 285–291.

[11] G. Dhatt, R. Song, A.N. Cheikh, Direct enthalpy method for solidification calculation, in: R. Gruber, et al. (Eds.), Proc. of the Fifth Int. Symp. on Numerical Methods in Engineering, Boston, 1989, pp. 487–494.

[12] G. Comini, S.D. Guidice, O. Saro, A conservative algorithm for multi-dimensional conduction phase change, Int. J. Numer. Methods Eng. 30 (1990) 697–709.

[13] V. Voller, C.R. Swaminathan, B.G. Thomas, Fixed grid techniques for phase change problems: a review, Int. J. Numer. Methods Eng. 30 (1990) 875–898.

[14] W.D. Murray, F. Landis, Numerical and machine solutions of transient heat conduction problem involving melting or freezing, ASME Trans. J. Heat Transfer 81 (1959) 106–112.

[15] L.A. Crivelli, S.R. Idelsohn, A temperature based finite element solution for phase-change problems, Int. J. Numer. Methods Eng. 23 (1986) 99–119.

[16] D. Celentano, E. Onate, S. Oller, A temperature-based formulation for finite element analysis of generalized phase-change problems, Int. J. Numer. Methods Eng. 37 (1994) 3441–3465.

[17] B.G. Thomas, I.V. Samarasekera, J.K. Brimacombe, Mathematical model of the thermal processing of steel ingots: part I, heat flow model, Metall. Trans. B 18 (1987) 119–130.

[18] S.D. Guidice, G. Comini, R.W. Lewis, Finite element simulation of freezing process in soils, Int. J. Numer. Anal. Methods Geomech. 2 (1978) 223–235.

[19] E.C. Lemmon, Phase change techniques for finite element codes, in: R.W. Lewis, K. Morgan (Eds.), Numerical Methods in Thermal Problems, Swansea, 1979, pp. 149–158.

[20] K. Tamma, R. Namburu, Recent advances, trends and new perspective via enthalpy-based finite element formulations for applications to solidification problems, Int. J. Numer. Methods Eng. 30 (1990) 803–820.

[21] U. Frisch, B. Hasslacher, Y. Pomeau, Lattice-gas automata for Navier–Stokes equations, Phys. Rev. Lett. 56 (1986) 1505–1508.

[22] S. Chen, G.D. Doolen, Lattice Boltzmann method for fluid flows, Annu. Rev. Fluid Mech. 30 (1998) 329–364.

[23] R. Benzi, S. Succi, M. Vergassola, The lattice Boltzmann equation: theory and applications, Phys. Rep. 222 (1992) 145–197.

[24] F. Higuera, S. Succi, R. Benzi, Lattice gas-dynamics with enhanced collisions, Europhys. Lett. 9 (1989) 345–349;
F.J. Higuera, J. Jimenez, Europhys. Lett. 9 (1989) 662–667.

[25] D. Wolf-Gladrow, Lattice-Gas Cellular Automata and Lattice Boltzmann Models: An Introduction, Springer-Verlag, Berlin–Heidelberg, 2000.

[26] S. Succi, The Lattice Boltzmann Equation for Fluid Dynamics and Beyond, Series Numerical Mathematics and Scientific Computation, Oxford–New York, Oxford Univ. Press, 2001.

[27] D. Wolf-Gladrow, A lattice Boltzmann equation for diffusion, J. Stat. Phys. 79 (1995) 1023–1032.

[28] G. de Fabritiis, A. Mancini, D. Mansutti, S. Succi, Mesoscopic models for melting/solidification processes, Int. J. Mod. Phys. C 9 (1998) 1405–1415.

[29] R.G.M. van der Sman, M.H. Ernst, A.C. Berkenbosch, Lattice Boltzmann scheme for cooling of packed cut flowers, Int. J. Heat Mass Transfer 43 (2000) 577–587.

[30] W. Miller, S. Succi, D. Mansutti, Lattice Boltzmann model for anisotropic liquid–solid phase transition, Phys. Rev. Lett. 86 (2001) 3578–3581.

[31] W.-S. Jiaung, J.-R. Ho, C.-P. Kuo, Lattice Boltzmann method for the heat conduction problem with phase change, Numer. Heat Transfer B 39 (2001) 167–187.

[32] P.L. Bhatnagar, E.P. Gross, M. Krook, A model for collision processes in charged and neutral one-component system, Phys. Rev. l94 (1954) 511–525.

[33] V. Sofonea, R.F. Sekerka, Viscosity of finite difference lattice Boltzmann models, J. Comp. Phys. 184 (2003) 422–434.

[34] A.D. Brent, V.R. Voller, K.J. Reid, Enthalpy–porosity technique for modelling convection–diffusion phase change: Application to the melting of a pure metal, Numer. Heat Transfer 13 (1988) 297–318.

[35] S. Chakraborty, P. Dutta, A generalised formulations for evaluation of latent heat functions in enthalpy-based macroscopic models for convection–diffusion phase change processes, Metall. Trans. B 32 (2001) 562–564.

[36] K.A. Rathjen, L.M. Jiji, Heat conduction with melting or freezing in a corner, ASME Trans. J. Heat Transfer 93 (1971) 101–109.

[37] R. Prapainop, K. Maneeratana, Simulation of ice formation by the finite volume method, Songklanakarin J. Sci. Technol. 26 (2004) 55–70.

[38] U. Hammerschmidt, Thermal transport properties of water and ice from one single experiment, in: Fourteenth Symposium on Thermophysical Properties, June 25–30, Boulder, CO, USA, 2000.